ACS OMEGA

http://pubs.acs.org/journal/acsodf

Article

BIRB796, an Inhibitor of p38 Mitogen-Activated Protein Kinase, Inhibits Proliferation and Invasion in Glioblastoma Cells

Linyao Zhao,[§] Yixuan Wang,[§] Yang Xu, Qian Sun, Hao Liu, Qianxue Chen,* and Baohui Liu*

Cite This: *ACS Omega* 2021, 6, 11466−11473

Read Online

ACCESS | Metrics & More | Article Recommendations

ABSTRACT: Glioblastoma (GBM) is the most common malignant tumor, and it is characterized by high cellular proliferation and invasion in the central nervous system of adults. Due to its high degree of heterogeneity and mortality, there is no effective therapy for GBM. In our study, we investigated the effect of the p38-MAPK signaling pathway inhibitor BIRB796 on GBM cells. Cell Counting Kit-8 (CCK-8) assay, 5-ethynyl-2′-deoxyuridine (EDU) staining, and cell cycle distribution analysis were performed, and the results showed that BIRB796 decreased proliferation in U87 and U251 cells. Moreover, wound healing and invasion assays were performed, which showed that BIRB796 inhibited the migration and invasion of human GBM cells. We found that BIRB796 treatment significantly decreased the formation of the cytoskeleton and thus downregulated the movement ability of the cells, as shown by phalloidin staining and vimentin immunofluorescence staining. Real-time polymerase chain reaction showed that the mRNA levels of MMP-2, Vimentin, CyclinD1, and Snail-1 were downregulated. Consistently, the expressions of MMP-2, Vimentin, CyclinD1, and p-p38 were also decreased after BIRB796 treatment. Taken together, all our results demonstrated that BIRB796 could play an antitumor role by inhibiting the proliferation and invasion in GBM cells. Thus, BIRB796 may be used as an adjuvant therapy to improve the therapeutic efficacy of GBM treatment.

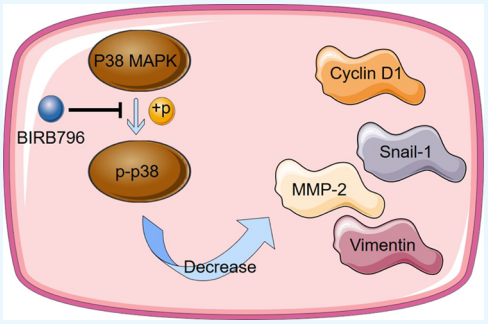

1. INTRODUCTION

Glioblastoma (GBM) is the most common primary tumor in the central nervous system of adults, and it is highly heterogeneous and difficult to cure.[1,2] Although multiple therapeutic strategies have been developed, including surgery, radiotherapy, and chemotherapy, the average survival time of glioblastoma patients remains less than 15 months. Despite the high number of research studies conducted, including genomic, transcriptomic, and epigenetic studies, the specific mechanism of GBM remains unknown.[3] However, emerging studies have demonstrated that p38-MAPK can influence different biological processes in GBM, such as the proliferation, invasion, and chemosensitivity of temozolomide.[4−6]

Among the mitogen-activated protein kinase (MAPK) pathways*, p38 pathway is a major pathway and was initially identified as a mediator of inflammation and stress responses.[7] p38 MAPK plays an extremely significant role in the key processes of cancer progression, such as proliferation, invasion, and survival.[8] Four isoforms of p38 MAPK (α, β, Υ, and δ) have shown tissue-specific expressions. The p38α is the most ubiquitously expressed isoform out of all the four isoforms.[9] Phosphorylation is one of the most common ways that lead to signaling of cell components that regulate proliferation[8] and invasion.[10] The p38 signaling inhibits proliferation and promotes cell death and thus is considered to suppress tumorigenesis.[11] For another, tumor cells can respond to microenvironment modifications and p38 signaling is a critical mechanism. Therefore, p38 signaling apparently has a dual function which not only facilitates cancer progression and resistance to chemotherapy but also suppresses tumorigenesis.[16] Due to this binary function as well as its dependance on the context, it is more than challenging to develop a potent antitumor therapeutic strategy to target the p38 MAPK pathway. In human GBM, p38 MAPK is upregulated,[10] whereas glioma cells showed a decline in the ability of invasion, both in vitro and in vivo, when p38 is inhibited. For another, an elevated susceptibility to apoptotic stimuli is also observed.[12] The p38 pathway is involved in reactive oxygen species (ROS) regulating glioma genesis and progression as well. ROS-mediated activation of p38 MAPK has an important role in controlling the differentiation and tumor-initiating capacity of glioma-initiating cells derived from human GBM.[13] p38 MAPK activity is elevated in human GBM specimens, and p38 MAPK inhibitors depress the secretion of proinflamma-

Received: January 28, 2021
Accepted: March 25, 2021
Published: April 22, 2021

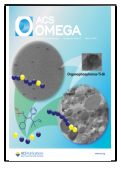

tory cytokines by microglia and GBM cells.[14] Thus, a potential anti-GBM strategy involves the blockade of the p38-MAPK signaling pathway.

BIRB-796 (also known as doramapimod) is one of the most potent compounds that targets a diaryl urea class allosteric binding site, indirectly competes with the binding of adenosine 5′-triphosphate (ATP), which is a novel mechanism in the inhibition of p38 and binds to p38 MAPK with high affinity.[15] BIRB-796 has been continuously studied over the years. It has been reported that BIRB-796 prevents p38α activation by upstream kinases[16] and improves cytotoxicity and inhibits paracrine tumor growth in multiple myeloma cell lines.[17] Moreover, in multidrug resistance protein ABCB1 over-expressing cells, He et al. demonstrated that BIRB-796 could strengthen the chemotherapy efficacy.[18] Jin et al. demonstrated that BIRB796 synergized with VX680 inhibited the growth of cervical cancer cells and activation of death pathways and may aid the design of novel targeted therapeutic regimens to achieve effective cancer treatments.[19] In this work, we first demonstrated that BIRB796 inhibited proliferation and invasion in GBM via the p38 MAPK signaling pathway. We used both U87 and U251 cell lines to test its inhibitory properties.

2. MATERIALS AND METHODS

2.1. Cell Culture. Human GBM cell lines (U87 and U251) were obtained from the cell bank, Shanghai Institutes for Biological Sciences, Chinese Academy of Sciences (Shanghai, China). The cells were cultured in high-glucose Dulbecco's modified Eagle's medium (DMEM) (Gibco Thermo Fisher Scientific, Inc, Waltham, MA, USA) supplemented with 10% fetal bovine serum (FBS) (Gibco Thermo Fisher Scientific, Inc, Waltham, MA, USA), 1% penicillin, and 1% streptomycin (Sigma-Aldrich; Merck KGaA, Darmstadt, Germany) at 37° C with 5% CO_2.

2.2. RNA Extraction and Quantitative Real-Time Polymerase Chain Reaction. Total RNA from cells was prepared using Trizol reagent (Invitrogen, USA), and cDNA was synthesized using a PrimeScript RT Reagent Kit with gDNA Eraser (RR047A, Takara, Japan). Quantitative real-time PCR (qPCR) for mRNA levels was performed using SYBR Premix Ex Taq II (RR820A, Takara) according to the manufacturer's instructions and performed in a Bio-Rad CFX Manager 2.1 real-time PCR Systems (Bio-Rad, USA). All the results were normalized to GAPDH. The data were analyzed by the relative Ct method and expressed as the fold change compared with the control. The sequences of primer are listed in Table 1.

2.3. Wound Healing Assays. U87 cells and U251 cells were seeded in 6-well plates (2×10^5 cells/well) and cultured until they reached 70−80% confluence. A wound was created by manually scraping the cell monolayer with a 200 μL pipette tip. The cells were washed with phosphate-buffered saline (PBS) and incubated in DMEM supplemented with 1% FBS. Cell migration was observed at three preselected time points (0, 24, and 48) by an Olympus BX51 microscope (magnification, ×100; Olympus BX51; Olympus, Tokyo, Japan). The area travelled by the cells could be quantitatively calculated using ImageJ Software (National Institutes of Health, Bethesda, MD, USA).

2.4. Transwell Assays. Transwell filters were coated with Matrigel in the top chamber of the QCM 24-Well Cell Invasion Assay (Cell Biolabs, Inc.). Approximately, 6×10^4 cells, treated with BIRB796, were plated on the top side of polycarbonate, which divided the medium without serum and the medium supplemented with serum to make a chemo-attractant in the chamber. The cells were incubated at 37 °C with 5% CO_2 for 24 h. The nonmigratory or noninvasive cells in the top chambers were removed with cotton swabs. The migrated cells on the lower membrane were fixed with 5% glutaraldehyde, stained with 0.5% crystal violet, and counted under a microscope (magnification, ×200; Olympus BX51; Olympus, Tokyo, Japan).

Table 1. qPCR Primer Sequences[a]

name	sequence (5′-3′)
GAPDH-F	GGAGCGAGATCCCTCCAAAAT
GAPDH-R	GGCTGTTGTCATACTTCTCATGG
MMP-2-F	CCCACTGCGGTTTTCTCGAAT
MMP-2-R	CAAAGGGGTATCCATCGCCAT
vimentin-F	AGTCCACTGAGTACCGGAGAC
vimentin-R	CATTTCACGCATCTGGCGTTC
snail-1-F	TCGGAAGCCTAACTACAGCGA
snail-1-R	AGATGAGCATTGGCAGCGAG
cyclin D1-F	CAATGACCCCGCACGATTTC
cyclin D1-R	CATGGAGGGCGGATTGGAA

[a]Abbreviations: F, forward; qPCR, quantitative PCR; R, reverse.

2.5. CCK-8 Assay. The cell viability was tested using a Cell Counting Kit-8 (CCK-8) (Dojindo, Shanghai, China), which determined the inhibitory effect of BIRB796 on the proliferation of U87 and U251 cells. Approximately 6×10^3 cells were seeded in each well of a 96-well plate and cultured with 0, 2, 4, 8, 16, 32, or 64 μM BIRB796 for either 24 or 48 h in 200 μL DMEM supplemented with 10% FBS. Then, the cells were incubated with 10 μL of CCK-8 for another 1 h. The absorbance at 450 nm of each well was measured by using a spectrophotometric plate reader. Assays of each group were tested in triplicate with three independent experiments.

2.6. Flow cytometry for Cell cycle Distribution Analysis. The effect of BIRB796 on the cell cycle distribution was detected by propidium iodide (PI) staining and flow cytometry. The cells, seeded in 6-well plates, were treated with 0, 8, 16, or 32 μM BIRB796 for 48 h. Then, the cells were fixed in cold 70% ethanol overnight at 4 °C and washed twice with PBS. Subsequently, 50 μL of 100 μg/mL RNase was added and incubated at 37 °C for 0.5 h and the cells were stained with 20 μL of PI from a 10 mg/mL stock solution. The results were analyzed using a flow cytometer (Becton-Dickinson, Franklin Lakes, NJ, USA); the data were analyzed using FlowJo software (version 7.6), and the data were quantified using ModFit LT 4.0 (http://www.vsh.com/products/mflt/index.asp; Verity Software House, Topsham, ME, USA).

2.7. 5-Ethynyl-2′-deoxyuridine Staining Assay. The assay was performed according to the manufacturer's protocol of the Cell-Light 5-ethynyl-2′-deoxyuridine (EdU) Apollo 643 In Vitro Imaging kit (100T), which was purchased from RiboBio Co., Ltd. (Guangzhou, China). Briefly, 5×10^3 cells were treated with 0, 8, 16, or 32 μM BIRB796 for 48 h and seeded with 100 μL of DMEM into each well of a 96-well plate. The cells were treated in the medium with 50 μM EdU for 12 h at 37 °C. After fixation with 4% paraformaldehyde for 30 min, the cells were treated with 0.5% Triton X-100 for 20 min. Next, 100 μL of the 1× Apollo reaction mixture was added to the cells for incubation for 30 min and 5 μg/mL Hoechst 33342 was used to stain the DNA for 30 min.

https://doi.org/10.1021/acsomega.1c00521
ACS Omega 2021, 6, 11466−11473

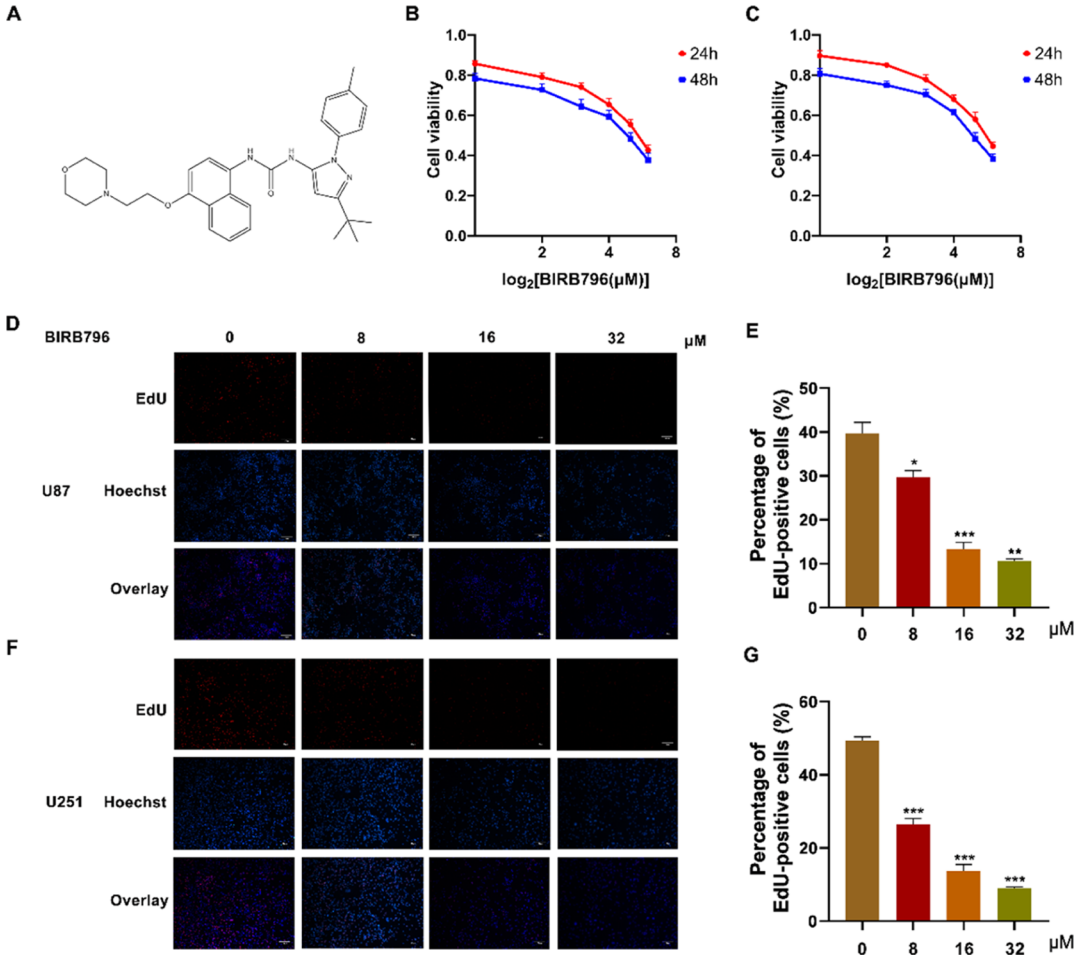

Figure 1. BIRB796 inhibits the proliferation of GBM cells in vitro. (A) Molecular structure of BIRB796. (B,C) Cell viability was measured with a CCK-8 assay after treatment of BRIB796 at various concentrations (0, 2, 4, 8, 16, 32, and 64 μM). (D−G) EdU assay showed that BIRB796 inhibited DNA synthesis in U87 and U251 cells in three independent experiments. *P < 0.05, **P < 0.01, and ***P < 0.001.

Fluorescence images were captured under a fluorescence microscope (magnification, ×200; Olympus BX51; Olympus, Tokyo, Japan).

2.8. Immunofluorescence. The cells were fixed in 4% paraformaldehyde for 15 min, permeabilized with 0.5% Triton X-100 for 10 min, and then blocked with 1% bovine serum albumin for 1 h. The cells were then incubated with the indicated primary antibodies overnight, followed by the Alexa Fluor-labelled secondary antibody (Antgene, Wuhan, China). The nuclei were stained with diamidino-2-phenylindole (DAPI) (ANT046, Antgene). The images were captured with the fluorescence microscope (magnification, ×200; Olympus BX51; Olympus, Tokyo, Japan).

2.9. Phalloidin Staining. The cells were fixed in 4% paraformaldehyde for 15 min, permeabilized with 0.1% Triton X-100 for 10 min, and then blocked with 1% bovine serum albumin for 0.5 h. The cells were then incubated with phalloidin (Antgene, Wuhan, China) for 2 h. The nuclei were stained with DAPI (ANT046, Antgene). The images were captured under the fluorescence microscope (magnification, ×x1000; Olympus BX51; Olympus, Tokyo, Japan).

2.10. Chemicals and Antibodies. BIRB796 was obtained from TargetMol (T6277, USA) and dissolved in dimethyl sulfoxide (DMSO), which was obtained from Merck KGaA. The antibodies were as follows: anti-p38 (#4511, Cell Signaling Technology, USA), anti-p-p38 (#9212, Cell Signaling Technology, USA), anti-GAPDH (#5174, Cell Signaling Technology, USA), anti-cyclin D1 (#2922, Cell Signaling Technology, USA), anti-MMP-2 (#4022, Cell Signaling Technology, USA), anti-Snail-1 (sc-393172, Santa Cruz Biotechnology, USA), anti-Vimentin (#5741, Cell Signaling Technology, USA), and Phalloidin (#12877, Cell Signaling Technology, USA).

2.11. Western Blotting. The cells were lysed in RIPA buffer (Beyotime, Shanghai, China) containing phenylmethylsulfonyl fluoride (Beyotime) and protease inhibitor cocktail (Roche) for 20 min at 4 °C and using the standard BCA method (Beyotime Institute of Biotechnology, Jiangsu, China) to assess the concentration of the proteins. Equal amounts of protein were separated by sodium dodecyl sulfate-polyacrylamide gel electrophoresis and transferred onto polyvinylidene difluoride membranes (Millipore, Germany). The membranes were blocked with BSA and then incubated with the indicated primary antibody overnight. Next, the membranes were incubated with Alexa Fluor 680/790-labeled secondary antibodies (LI-COR Bioscience, USA) for 2 h. The bands were visualized with a BioRad Infrared Imaging System (LI-COR Biosciences, Lincoln, NE, USA) for 2 h. Densitometry analyses were performed with Quantity One (BioRad, USA). The results were normalized to GAPDH and visualized using the LI-COR Odyssey Infrared Imaging System.

https://doi.org/10.1021/acsomega.1c00521
ACS Omega 2021, 6, 11466−11473

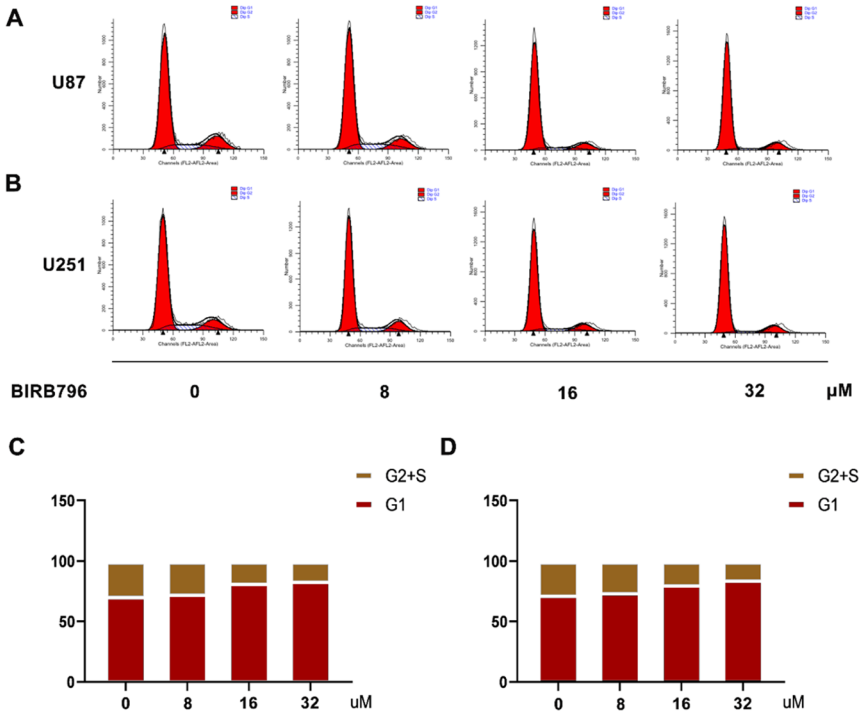

Figure 2. BIRB796 blocks the cell cycle at G1 phase in GBM cells. (A,B) Cell accumulation at G1/G2+S phase after treatment with BIRB796 for 24 h measured by flow cytometry. (C,D) Results were visualized.

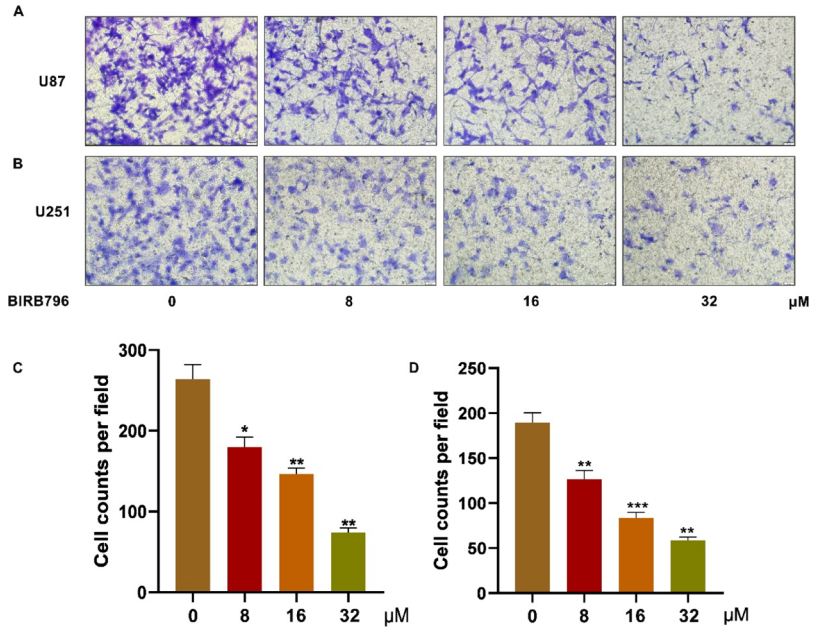

Figure 3. BIRB796 inhibits the migration of GBM cells. (A,C) Wound healing assay showed the migration ability of U87 and U251 cells treated with BIRB796 at different concentrations (0, 8, 16, and 32 μM); (B,D) rate of wound closure of U87 and U251 cells after treatment with BIRB796. *P < 0.05, **P < 0.01, and ***P < 0.001.

2.12. Statistical Analysis. All results are representative of three independent experiments and presented as the mean ± SD. Statistical analyses were performed with SPSS version 19.0 and GraphPad Prism 8. Unpaired Student's t-tests were used to compare the means of two groups. One-way analysis of variance was used for comparisons among the different groups. When analysis of variance was significant, post hoc testing of differences between groups was performed using Student–Newman–Keuls test. The results were considered significant at *P < 0.05, **P < 0.01, and ***P < 0.001.

3. RESULTS

3.1. BIRB796 Inhibits the Proliferation of U87 and U251 Cells. The chemical formula of BIRB796 is shown in Figure 1A. To confirm the antiproliferative effect of BIRB796 on U87 and U251 cells, we performed the CCK-8 assay. The two cell lines were exposed to different concentrations of

https://doi.org/10.1021/acsomega.1c00521
ACS Omega 2021, 6, 11466−11473

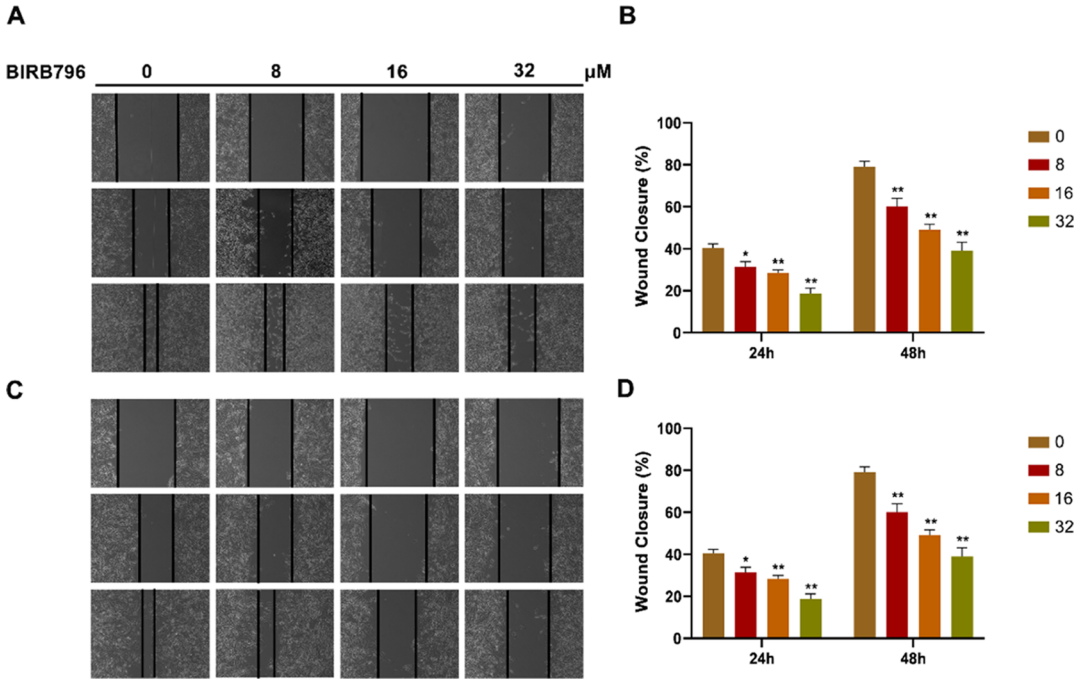

Figure 4. BIRB796 inhibits the migration and invasion of GBM cells. (A,B) Transwell assays were performed to detect the migration and invasion ability of U87 and U251 cells treated with BIRB796 at different concentrations (0, 8, 16, and 32 μM); (C,D) quantification of the results of (A,B). Results represent at least three independent experiments. *P < 0.05, **P < 0.01, and ***P < 0.001.

BIRB796 (including 0−64 μM) for 24 and 48 h. The inhibitory effects on both cell lines showed dose-dependent and time-dependent effects (Figure 1B,C). The IC_{50} values of BIRB796 were 34.96 μM and 46.30 μM in U87 and U251 cells, respectively. Furthermore, to detect the potential inhibitory effect of BIRB796, we performed a EdU incorporation assay in both U87 and U251 cells. The fluorescence images showed that the percentage of EdU-positive cells was significantly decreased at different concentrations (Figure 1D−G), indicating that DNA replication was inhibited by BIRB796. These results demonstrated an antiproliferative effect of BIRB796 on GBM cells.

3.2. BIRB796 Blocks the Cell Cycle at the G1 Phase in U87 and U251 Cells. The viability of cells is related to the cell cycle. The cells treated with different concentrations of BIRB796 for 48 h were stained with PI and analyzed by flow cytometry. The results showed that BIRB796 blocked the G1 phase cell cycle arrest in U87 cells (Figure 2A,C). In addition, S and G2 phases significantly declined. The same results were seen with U251 cells (Figure 2B,D). Moreover, it has been reported that p38 MAPK regulates the expression of CyclinD1. We detected the mRNA and protein levels of CyclinD1, and the results showed a declined level of CyclinD1, which is consistent with the level of p-p38 after BIRB796 treatment (Figure 6).

3.3. BIRB796 Inhibits the Migration and Invasion of U87 and U251 Cells. We performed wound-healing and invasion assays in U251 and U87 cells at various concentrations (0, 8, 16, and 32 μM) to detect the potential effect of BIRB796 on GBM invasion. The results showed that the growth rate of the area became slower with increasing concentrations in both U87 and U251 cells (Figure 3). Consistent with these results, the invasive ability of the cells reduced significantly with higher concentrations of BIRB796 in the Transwell invasion assay (Figure 4). Furthermore, we detected that the mRNA and protein levels of MMP-2 and Snail-1 decreased along with the decline in p-p38 after BIRB796 treatment (Figure 6). All of the results demonstrated that BIRB796 inhibited the migration and invasion of U87 and U251 cells.

3.4. BIRB796 Decreased the Cytoskeleton of U87 and U251 Cells. To further assess cell movement, we performed phalloidin staining and immunofluorescent staining of vimentin. The cells treated with RIRB796 showed a significant reduction in the cytoskeleton compared with the untreated group through phalloidin and vimentin staining in both U251 and U87 cells (Figure 5A,B). Consistently, the fluorescence intensity of vimentin decreased obviously between the treated and the untreated groups. Meanwhile, we performed PCR and Western blotting to test the mRNA and protein levels of vimentin and found positive correlation between vimentin and p-p38 (Figure 6). All of the results demonstrated that BIRB796 decreased the cytoskeleton of U87 and U251 cells.

4. DISCUSSION

GBM is one of the most malignant primary tumors in the central nervous system and has high mortality and morbidity rates. The P38-MAPK pathway plays a complicated role in different cancers, and phosphorylated-p38 can be used as a possible biomarker of glioma progression due to its positive correlation with tumor grades.[20] Meanwhile, it has been reported that the inhibitors targeting the p38-MAPK pathway have the capacity to sensitize arrested GBM cells to cytotoxic therapy.[10] Targeted p38 inhibitors are potential anticancer drugs, and BIRB796 is an inhibitor indirectly competing with the binding of ATP with high affinity.[15] However, the accurate role of BIRB796 in GBMs has remained unclear.

In the present study, we confirmed that BIRB796 inhibited the proliferation of U251 and U87 cells by promoting G1 arrest. The p38-MAPK pathway has been demonstrated to be a

https://doi.org/10.1021/acsomega.1c00521
ACS Omega 2021, 6, 11466−11473

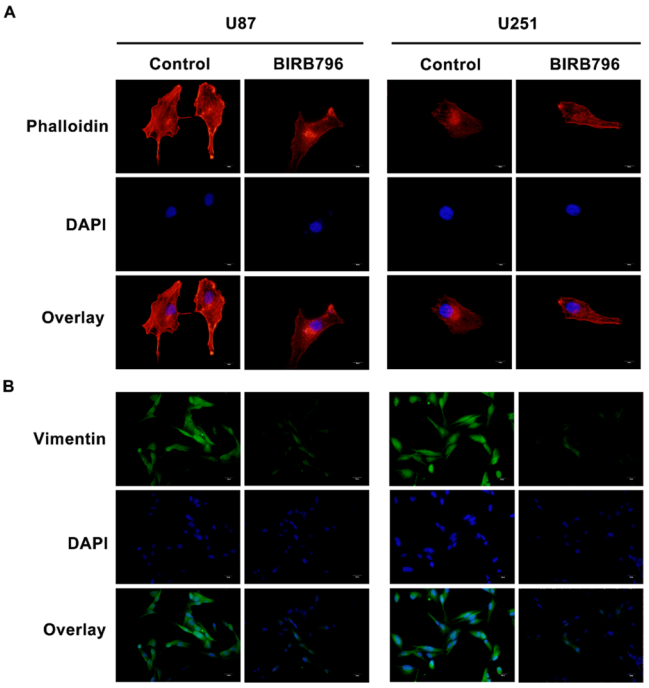

Figure 5. BIRB796 decreased the cytoskeleton of GBM cells. (A) Phalloidin staining of U87 and U251 cells. The cytoskeleton was remarkably decreased after treatment with BIRB796. (B) Fluorescent images of Vimentin in U87 and U251 cells.

regulator of checkpoint, which controls the cell cycle at G0, G1/S, and G2/M transitions.[21] Among these pathways, the p38-MAPK pathway can either induce progression or inhibit G1/S transition by either regulating specific cyclin levels or phosphorylation of the retinoma protein, depending on the cell cycle progression.[22] The cyclin-CDK complex and CDK inhibitor proteins play a critical role in the cell cycle. Cyclin D1 forms a complex with CDK4, which is a significant regulator of the G1/S checkpoint to promote cellular passage to the G1 phase.[23] Previous studies have demonstrated that inactivation of the P38-MAPK pathway decreases the expression of CyclinD1.[24,25] Consistently, the expression of CyclinD1 also declined after BIRB796 treatment in our study, and the G1 arrest of U251 and U87 cells was probably caused by the blockade effect of BIRB796 in the P38-MAPK pathway.

In our study, the results showed that BIRB796 significantly inhibited the migration and invasion of GBM cells. Matrix metalloproteinases (MMPs) play an important role in tissue remodeling associated with various physiological or pathological processes. The amplifying impact of MMPs derived from cancer is the beginning of cancer pathogenesis and promotes cell proliferation, angiogenesis, invasion, and metastasis through the degradation of the extracellular matrix.[26] Moreover, it has been reported that inactivity of the p38 signaling pathway reduces the modulation of the migration and invasion via the reduction of MMP-2 in glioma cells.[27] To confirm the potential molecular mechanism, we performed PCR and Western blotting of MMP-2 and detected a decrease in the expression level. Furthermore, vimentin is an intermediate filament that regulates cell attachment and

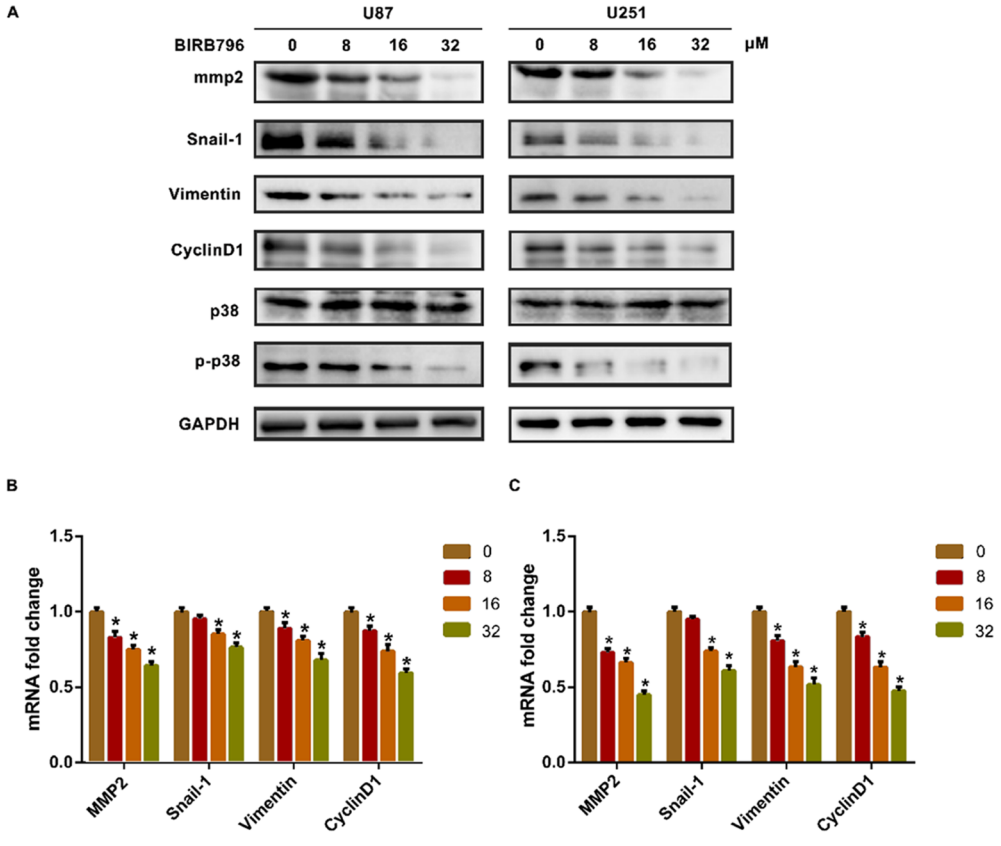

Figure 6. BIRB796 inhibited proliferation and invasion in GBM cells. (A) Western blotting assay of protein expression after BIRB796 treatment. (B,C) Q-PCR results of mRNA fold change of MMP-2, Snail-1, Vimentin, and Cyclin D1 in U87 and U251 cells.

https://doi.org/10.1021/acsomega.1c00521
ACS Omega 2021, 6, 11466−11473

subcellular organization and surrounds the nucleus, extending outward to the cell periphery.[28] It has been reported that activation of p38-MAPK signaling enhances the expression of several epithelial−mesenchymal transition markers, such as slug and vimentin.[29] The results of vimentin immunofluorescence showed that the intensity of immunofluorescence decreased obviously after BIRB796 treatment. To test the results further, we performed PCR and Western blotting. The results showed that the mRNA and protein levels of vimentin decreased as the concentration of BIRB796 increased. Furthermore, p38 also plays a role in cytoskeletal remodeling. It has been demonstrated that the activation of the p38-MAPK signaling pathway stimulates the phosphorylation of the small heat shock protein HspB1 (also known as mouse hsp25 and human hsp27) and recruits it to the actin cytoskeleton.[30] To confirm the effect of BIRB796 on the cytoskeleton, we performed phalloidin staining, which showed that the cytoskeleton was significantly decreased after treatment with BIRB796. This phenomenon further elucidated that BIRB796 inhibited migration and invasion not only through the inhibition of MMP-2 but also through cytoskeletal remodeling.

Although we have obtained some notable results that demonstrate the effects of BIRB796, the present study still has several limitations. First, we only detected the effect of BIRB796, and it has been reported that BIRB796 inhibits not only p38α and p38β but also p38γ and p38δ at higher concentrations.[31] However, we did not examine the specific isoforms of p38 taking effects in this study. Furthermore, we only performed our studies using U87 and U251 cells, and the effect of BIRB796 on GBMs was not examined in vivo; however, our research also provides enough evidence for the experiments used in GBM. Finally, we did not have sufficient clinical evidence to demonstrate our results. We need to do further research in the future. Nonetheless, our results are credible and could provide a promising drug candidate for GBM therapy.

5. CONCLUSIONS

In conclusion, our study illustrated for the first time that BIRB796 can inhibit proliferation and invasion capabilities in human GBM cells. These findings reveal a new potential therapeutic application of BIRB796 in the treatment of GBM.

AUTHOR INFORMATION

Corresponding Authors

Qianxue Chen − *Department of Neurosurgery, Renmin Hospital of Wuhan University, Hubei 430060, China; Central Laboratory, Renmin Hospital of Wuhan University, Wuhan, Hubei 430060, PR China*; Email: chenqx666@whu.edu.cn

Baohui Liu − *Department of Neurosurgery, Renmin Hospital of Wuhan University, Hubei 430060, China; Central Laboratory, Renmin Hospital of Wuhan University, Wuhan, Hubei 430060, PR China*; orcid.org/0000-0001-5821-6945; Email: bliu666@whu.edu.cn

Authors

Linyao Zhao − *Department of Neurosurgery, Renmin Hospital of Wuhan University, Hubei 430060, China; Central Laboratory, Renmin Hospital of Wuhan University, Wuhan, Hubei 430060, PR China*

Yixuan Wang − *Department of Neurosurgery, Renmin Hospital of Wuhan University, Hubei 430060, China; Central Laboratory, Renmin Hospital of Wuhan University, Wuhan, Hubei 430060, PR China*

Yang Xu − *Department of Neurosurgery, Renmin Hospital of Wuhan University, Hubei 430060, China; Central Laboratory, Renmin Hospital of Wuhan University, Wuhan, Hubei 430060, PR China*

Qian Sun − *Department of Neurosurgery, Renmin Hospital of Wuhan University, Hubei 430060, China; Central Laboratory, Renmin Hospital of Wuhan University, Wuhan, Hubei 430060, PR China*

Hao Liu − *Department of Neurosurgery, Renmin Hospital of Wuhan University, Hubei 430060, China; Central Laboratory, Renmin Hospital of Wuhan University, Wuhan, Hubei 430060, PR China*

Complete contact information is available at: https://pubs.acs.org/10.1021/acsomega.1c00521

Author Contributions

[§]L.Z. and Y.W. contributed equally to this study and should be considered joint authors.

Notes

The authors declare no competing financial interest.

The data used to support the findings of this study are available from the corresponding author upon request.

ACKNOWLEDGMENTS

This work was supported by the National Natural Science Foundation of China (nos. 81572489, 81372683, and 81502075).

REFERENCES

(1) Louis, D. N.; Perry, A.; Reifenberger, G.; von Deimling, A.; Figarella-Branger, D.; Cavenee, W. K.; Ohgaki, H.; Wiestler, O. D.; Kleihues, P.; Ellison, D. W. The 2016 World Health Organization Classification of Tumors of the Central Nervous System: a summary. *Acta Neuropathol.* **2016**, *131*, 803−820.

(2) Ostrom, Q. T.; Gittleman, H.; Truitt, G.; Boscia, A.; Kruchko, C.; Barnholtz-Sloan, J. S. CBTRUS Statistical Report: Primary Brain and Other Central Nervous System Tumors Diagnosed in the United States in 2011-2015. *Neuro-Oncology* **2018**, *20*, iv1−iv86.

(3) Aldape, K.; Zadeh, G.; Mansouri, S.; Reifenberger, G.; von Deimling, A. Glioblastoma: pathology, molecular mechanisms and markers. *Acta Neuropathol.* **2015**, *129*, 829−848.

(4) Wirthschaft, P.; Bode, J.; Simon, A. E. M.; Hoffmann, E.; van Laack, R.; Krüwel, T.; Dietrich, F.; Bucher, D.; Hahn, A.; Sahm, F.; Breckwoldt, M. O.; Kurz, F. T.; Hielscher, T.; Fischer, B.; Dross, N.; Ruiz de Almodovar, C.; von Deimling, A.; Herold-Mende, C.; Plass, C.; Boulant, S.; Wiestler, B.; Reifenberger, G.; Lichter, P.; Wick, W.; Tews, B. A PRDX1-p38α heterodimer amplifies MET-driven invasion ofIDH-wildtype andIDH-mutant gliomas. *Int. J. Cancer* **2018**, *143*, 1176−1187.

(5) Ma, L.; Liu, J.; Zhang, X.; Qi, J.; Yu, W.; Gu, Y. p38 MAPK-dependent Nrf2 induction enhances the resistance of glioma cells against TMZ. *Med. Oncol.* **2015**, *32*, 69.

(6) Chen, Y.; Gao, F.; Jiang, R.; Liu, H.; Hou, J.; Yi, Y.; Kang, L.; Liu, X.; Li, Y.; Yang, M. Down-Regulation of AQP4 Expression via p38 MAPK Signaling in Temozolomide-Induced Glioma Cells Growth Inhibition and Invasion Impairment. *J. Cell. Biochem.* **2017**, *118*, 4905−4913.

(7) Ono, K.; Han, J. The p38 signal transduction pathway: activation and function. *Cell. Signalling* **2000**, *12*, 1−13.

(8) Wagner, E. F.; Nebreda, Á. R. Signal integration by JNK and p38 MAPK pathways in cancer development. *Nat. Rev. Cancer* **2009**, *9*, 537−549.

(9) Zarubin, T.; Han, J. Activation and signaling of the p38 MAP kinase pathway. *Cell Res.* **2005**, *15*, 11−18.
(10) Demuth, T.; Reavie, L. B.; Rennert, J. L.; Nakada, M.; Nakada, S.; Hoelzinger, D. B.; Beaudry, C. E.; Henrichs, A. N.; Anderson, E. M.; Berens, M. E. MAP-ing glioma invasion: mitogen-activated protein kinase kinase 3 and p38 drive glioma invasion and progression and predict patient survival. *Mol. Cancer Ther.* **2007**, *6*, 1212−1222.
(11) Bulavin, D. V.; Fornace, A. J., Jr. p38 MAP kinase's emerging role as a tumor suppressor. *Adv. Cancer Res.* **2004**, *92*, 95−118.
(12) Stupp, R.; Mason, W. P.; van den Bent, M. J.; Weller, M.; Fisher, B.; Taphoorn, M. J. B.; Belanger, K.; Brandes, A. A.; Marosi, C.; Bogdahn, U.; Curschmann, J.; Janzer, R. C.; Ludwin, S. K.; Gorlia, T.; Allgeier, A.; Lacombe, D.; Cairncross, J. G.; Eisenhauer, E.; Mirimanoff, R. O.; European Organisation for, R.; Treatment of Cancer Brain, T.; Radiotherapy, G. Radiotherapy plus Concomitant and Adjuvant Temozolomide for Glioblastoma. *N. Engl. J. Med.* **2005**, *352*, 987−996.
(13) Sato, A.; Okada, M.; Shibuya, K.; Watanabe, E.; Seino, S.; Narita, Y.; Shibui, S.; Kayama, T.; Kitanaka, C. Pivotal role for ROS activation of p38 MAPK in the control of differentiation and tumor-initiating capacity of glioma-initiating cells. *Stem Cell Res.* **2014**, *12*, 119−131.
(14) Yeung, Y. T.; Bryce, N. S.; Adams, S.; Braidy, N.; Konayagi, M.; McDonald, K. L.; Teo, C.; Guillemin, G. J.; Grewal, T.; Munoz, L. p38 MAPK inhibitors attenuate pro-inflammatory cytokine production and the invasiveness of human U251 glioblastoma cells. *J Neurooncol.* **2012**, *109*, 35−44.
(15) Pargellis, C.; Tong, L.; Churchill, L.; Cirillo, P. F.; Gilmore, T.; Graham, A. G.; Grob, P. M.; Hickey, E. R.; Moss, N.; Pav, S.; Regan, J. Inhibition of p38 MAP kinase by utilizing a novel allosteric binding site. *Nat. Struct. Biol.* **2002**, *9*, 268−272.
(16) Sullivan, J. E.; Holdgate, G. A.; Campbell, D.; Timms, D.; Gerhardt, S.; Breed, J.; Breeze, A. L.; Bermingham, A.; Pauptit, R. A.; Norman, R. A.; Embrey, K. J.; Read, J.; VanScyoc, W. S.; Ward, W. H. J. Prevention of MKK6-Dependent Activation by Binding to p38α MAP Kinase‡. *Biochemistry* **2005**, *44*, 16475−16490.
(17) Yasui, H.; Hideshima, T.; Ikeda, H.; Jin, J.; Ocio, E. M.; Kiziltepe, T.; Okawa, Y.; Vallet, S.; Podar, K.; Ishitsuka, K.; Richardson, P. G.; Pargellis, C.; Moss, N.; Raje, N.; Anderson, K. C. BIRB 796 enhances cytotoxicity triggered by bortezomib, heat shock protein (Hsp) 90 inhibitor, and dexamethasone via inhibition of p38 mitogen-activated protein kinase/Hsp27 pathway in multiple myeloma cell lines and inhibits paracrine tumour growth. *Br. J. Haematol.* **2007**, *136*, 414−423.
(18) He, D.; Zhao, X.-q.; Chen, X.-g.; Fang, Y.; Singh, S.; Talele, T. T.; Qiu, H.-j.; Liang, Y.-j.; Wang, X.-k.; Zhang, G.-q.; Chen, Z.-s.; Fu, L.-w. BIRB796, the inhibitor of p38 mitogen-activated protein kinase, enhances the efficacy of chemotherapeutic agents in ABCB1 overexpression cells. *PLoS One* **2013**, *8*, No. e54181.
(19) Jin, X.; Mo, Q.; Zhang, Y.; Gao, Y.; Wu, Y.; Li, J.; Hao, X.; Ma, D.; Gao, Q.; Chen, P. The p38 MAPK inhibitor BIRB796 enhances the antitumor effects of VX680 in cervical cancer. *Canc. Biol. Ther.* **2016**, *17*, 566−576.
(20) Glassmann, A.; Reichmann, K.; Scheffler, B.; Glas, M.; Veit, N.; Probstmeier, R. Pharmacological targeting of the constitutively activated MEK/MAPK-dependent signaling pathway in glioma cells inhibits cell proliferation and migration. *Int. J. Oncol.* **2011**, *39*, 1567−1575.
(21) Ambrosino, C.; Nebreda, A. R. Cell cycle regulation by p38 MAP kinases. *Biol. Cell.* **2001**, *93*, 47−51.
(22) Brancho, D.; Tanaka, N.; Jaeschke, A.; Ventura, J. J.; Kelkar, N.; Tanaka, Y.; Kyuuma, M.; Takeshita, T.; Flavell, R. A.; Davis, R. J. Mechanism of p38 MAP kinase activation in vivo. *Genes Dev.* **2003**, *17*, 1969−1978.
(23) Malumbres, M.; Barbacid, M. Cell cycle, CDKs and cancer: a changing paradigm. *Nat. Rev. Cancer* **2009**, *9*, 153−166.
(24) Li, L.; Dang, Y.; Zhang, J.; Yan, W.; Zhai, W.; Chen, H.; Li, K.; Tong, L.; Gao, X.; Amjad, A.; Ji, L.; Jing, T.; Jiang, Z.; Shi, K.; Yao, L.; Song, D.; Liu, T.; Yang, X.; Yang, C.; Cai, X.; Xu, W.; Huang, Q.; He, J.; Liu, J.; Chen, T.; Moses, R. E.; Fu, J.; Xiao, J.; Li, X. REGgamma is critical for skin carcinogenesis by modulating the Wnt/beta-catenin pathway. *Nat. Commun.* **2015**, *6*, 6875.
(25) Hsu, M. K. H.; Qiao, L.; Ho, V.; Zhang, B.-H.; Zhang, H.; Teoh, N.; Dent, P.; Farrell, G. C. Ethanol reduces p38 kinase activation and cyclin D1 protein expression after partial hepatectomy in rats. *J. Hepatol.* **2006**, *44*, 375−382.
(26) Curran, S.; Murray, G. I. Matrix metalloproteinases: molecular aspects of their roles in tumour invasion and metastasis. *Eur. J. Canc.* **2000**, *36*, 1621−1630.
(27) Liu, Y.; Zheng, J.; Zhang, Y.; Wang, Z.; Yang, Y.; Bai, M.; Dai, Y. Fucoxanthin Activates Apoptosis via Inhibition of PI3K/Akt/mTOR Pathway and Suppresses Invasion and Migration by Restriction of p38-MMP-2/9 Pathway in Human Glioblastoma Cells. *Neurochem. Res.* **2016**, *41*, 2728−2751.
(28) Owen, P. J.; Johnson, G. D.; Lord, J. M. Protein kinase C-delta associates with vimentin intermediate filaments in differentiated HL60 cells. *Exp. Cell Res.* **1996**, *225*, 366−373.
(29) Lu, L.; Wang, J.; Wu, Y.; Wan, P.; Yang, G. Rap1A promotes ovarian cancer metastasis via activation of ERK/p38 and notch signaling. *Cancer Med.* **2016**, *5*, 3544−3554.
(30) Hoffman, L.; Jensen, C. C.; Yoshigi, M.; Beckerle, M. Mechanical signals activate p38 MAPK pathway-dependent reinforcement of actin via mechanosensitive HspB1. *Mol. Biol. Cell* **2017**, *28*, 2661−2675.
(31) Kuma, Y.; Sabio, G.; Bain, J.; Shpiro, N.; Márquez, R.; Cuenda, A. BIRB796 inhibits all p38 MAPK isoforms in vitro and in vivo. *J. Biol. Chem.* **2005**, *280*, 19472−19479.

https://doi.org/10.1021/acsomega.1c00521
ACS Omega 2021, 6, 11466−11473